Maintenance, Safety, Risk, Management and Life-Cycle Performance of Bridges – Powers, Frangopol, Al-Mahaidi & Caprani (Eds)
© 2018 Taylor & Francis Group, London, ISBN 978-1-138-73045-8

Reliability Assessment of Reinforced Concrete Pylons Subjected to Biaxial Bending

Ji Hyeon Kim & Hae Sung Lee
Seoul National University, Seoul, Republic of Korea

ABSTRACT: This paper presents the reliability assessment of reinforced concrete pylons for cable-supported bridges subjected to biaxial bending moment. The load contour method is employed to determine the strength of reinforced concrete pylons under biaxial bending. The failure surface defined by the load contour method is utilized as the limit state function in the reliability analysis. The load parameter and the strength parameter such as the material and geometric properties are considered as random variables. The most probable failure point and reliability index are calculated by the Hasofer-Lind Rackwitz-Fiessler algorithm with the gradient projection method for the advanced first-order second-moment reliability method. The reliability analyses of the pylon for cable-supported bridges in Korea are performed for the surface exponents of 1 and 2. The effect of the surface exponents and the comparison of the reliability index for uniaxial bending to that for biaxial bending are discussed in detail.

1 INTRODUCTION

A robust reliability assessment method of reinforced concrete (RC) columns subjected to biaxial bending is proposed by Kim and Lee (2017). The proposed method is utilized to evaluate a reliability level of rectangular sections for short columns in the study. The proposed scheme certainly plays an important role for code calibration procedure, in which the reliability indices for various real sections should be evaluated to set a target reliability index. The reliability levels of RC pylons need to be estimated accurately to determine a proper a target reliability index of a wind load-governed limit state for cable-supported bridges.

As a cross-section of the pylons for cable-supported bridges is usually designed as a hollow section, the section properties for internal forces have to be estimated based on the effective flange width considering the shear lag or determined by rigorous analysis. However, most design codes (AASHTO, 2012; KMOLIT, 2016a; KMOLIT, 2016b) state that the full compression flange width effect is valid for the capacity of a cross-section at the strength limit state. The scope of this study is to estimate the reliability index of an RC pylon for the strength limit state, and thus, the entire cross-section is valid to evaluate the strength of RC pylons.

This paper adopts the reliability assessment method proposed by Kim and Lee (2017) in order to estimate reliability levels of RC pylons for cable-supported bridges subjected to biaxial bending. The failure surface defined in the load contour method is provided as the limit state function for the reliability analysis. The minimization problem defined by the advanced-first order second-moment reliability method (AFOSM) (Haldar and Mahadevan, 2000) is solved by using the Hasofer-Lind Rackwitz-Fiessler (HL-RF) algorithm with the gradient projection method (Liu and Der Kiureghain, 1991). The axial force (P) - bending moment (M) interaction diagram (PMID) of a pylon under uniaxial bending is interpolated by using the cubic spline method as presented in Kim et al. (2015). The PMIDs about the principal axes of the section are used in constructing the load contour. The sensitivities of the limit state function required in the HL-RF algorithm are calculated through the direct differentiation method.

The reliability indexes and most probable failure points (MPFPs) of the pylon for cable-supported bridges in Korea are calculated in case that the surface exponents of the load contour are 1 and 2. The effect of the surface exponents are investigated through the reliability analyses. The reliability index of RC pylons subjected to uniaxial bending is compared to the reliability index under biaxial bending. It is demonstrated that the reliability index of a pylon for biaxial bending may become significantly lower than that for uniaxial bending depending on the surface exponent.

2 RELIABILITY ASSESSMENT METHOD

2.1 *3-dimensional PMID*

Kim and Lee (2017) adopts the load contour method proposed by Bresler (1980) in order to define the PMID of an RC column subject to combined axial and biaxial bending moment in the 3-dimensional axial force (P)-moments (M_y, M_z) space.

$$\Phi(\mathbf{F},\mathbf{B}) = \Phi(P, M_z, M_y, \mathbf{B})$$
$$= 1 - \left(\frac{M_y}{\widetilde{M}_y(P)}\right)^{\alpha} - \left(\frac{M_z}{\widetilde{M}_z(P)}\right)^{\alpha} = 0 \quad (1)$$

where $\mathbf{F} = (P, M_y, M_z)^T$, $\mathbf{B}$ is the surface parameter vector of the PMID, and α is the surface exponent that is determined by the strength characteristic of a cross section. M_y and M_z represents the y-directional and z-directional moments, respectively. $\widetilde{M}_y(P)$ and $\widetilde{M}_z(P)$ are the ultimate moment capacities for a given P in pure bending about the y and z direction, respectively. The surface exponent, α, determines the feasible region of the load contours that present the PMID in $M_y - M_z$ plane. The α of 1 indicates the lower limit of the columns strength and describes a straight line connecting the $\widetilde{M}_y(P)$ and $\widetilde{M}_z(P)$. The α of 2 denotes the upper limit of the column strength and the load contours are drawn as the ellipse.

The PMIDs of the column subject to the y and z directional uniaxial bending moment are expressed in terms of the axial force, respectively, and are defined in the $P - M_y$ plane and the $P - M_z$ plane as follows:

$$\Phi_k(P, \widetilde{M}_k, \mathbf{B}_k) = 0 \quad \text{for} \quad k = y, z \quad (2)$$

The subscript k indicates the direction of the uniaxial bending moment hereafter.

The limit state of an RC column is defined by the PMID given in Eq. (1) and described as $\Phi(\mathbf{F}_q, \mathbf{B}) = 0$. That is, $\Phi(\mathbf{F}_q, \mathbf{B}) > 0$ and $\Phi(\mathbf{F}_q, \mathbf{B}) < 0$ represent the safe and failure states of the RC column, respectively. $\mathbf{F}_q$ denotes the internal force vector. The relations between the internal forces and the external loads are assumed to be linear, although each external load component may have nonlinear load effects on an RC column.

$$\mathbf{F}_{q,0} = \begin{pmatrix} P_q \\ M_{q,y} \\ M_{q,z} \end{pmatrix} = \mathbf{C}_0 \mathbf{q} \quad (3)$$

Here, $\mathbf{C}_0$ and $\mathbf{q}$ are the load effect matrix and load parameter vector, respectively. Each column of the load effect matrix is composed of the load effects calculated in the structural analysis for the nominal value of the corresponding load component. The load parameter vector represents the statistical properties of the load components. The nominal values of the load parameters are given as 1, and the mean value of each load parameter becomes the bias factor of the original load component. The statistical distribution and coefficient of variation (COV) of each load parameter follow those of the original load component.

The surface parameters are determined based on the strength parameters representing the material and geometric properties of a cross section. The strength parameters of an RC column are conveniently written in one vector

$$\mathbf{s} = (s_j)$$
$$= (f_{ck}, f_y, E_s, A_{gt}, A_{s,1}, \ldots, A_{s,m}, y_{s,1}, \ldots, y_{s,m}, z_{s,1}, \ldots, z_{s,m})^T \quad (4)$$

where f_{ck}, f_y, E_s indicate the compressive strength of concrete, the yield strength of the reinforcing bar and the Young's modulus of the reinforcing bar, respectively, and are included in the material properties. m, A_{gt}, $A_{s,k}$, $y_{s,k}$, $z_{s,k}$ denote the number of reinforcing bars, the gross area of a cross section, the area and position of the k-th reinforcing bar in the y and z direction, respectively. he position of a reinforcing bar is the distance from the extreme compression fiber of the cross section to the center of the reinforcing bar. The geometric properties consist of the area and position of each reinforcing bar and the gross area of a cross section.

The PMID of $P - M_k$ plane is composed of infinite sampling points, which represent the ultimate strength combinations of RC Columns. Kim et al. (2015) suggested the analytic form of the PMID in $P - M_k$ plane by introducing a piecewise cubic polynomial functions (Kreyzig, 2006). The polynomial function, called as the cubic spline, is used to interpolate two adjacent points as a piecewise continuous and twice differentiable function.

2.2 *AFOSM*

The strength parameters of an RC column, the load parameters are considered to be random variables. All random variables are assumed to be statistically independent to each other in this study. For the compactness of forthcoming derivations, the random variables are written in one vector, $\mathbf{X} = (\mathbf{q}, \mathbf{s})^T$. In case that all random variables are normally distributed and statistically independent to each other, the reliability index and corresponding MPFP are evaluated by solving the following minimization problem through the AFOSM (Haldar and Mahadevan, 2000):

$$\underset{\overline{\mathbf{X}}}{\mathrm{Min}}\, \beta^2 = \left\|\overline{\mathbf{X}}\right\|_2^2 \quad \text{subject to} \quad \overline{\Phi}(\overline{\mathbf{X}}) = 0 \quad (5)$$

where β and $\|\cdot\|_2$ denote the reliability index and the 2-norm of a vector, respectively, while the overbarred variables indicate standardized random variables and $\overline{\Phi}(\overline{\mathbf{X}}) = \Phi(\mathbf{X})$. Since the limit state function is nonlinear with respect to the random variables, the minimization problem given in Eq. (5) is solved iteratively by the HL-RF algorithm with the gradient projection method (Liu and Der Kiureghain, 1991). The Rackwitz-Fiessler method (Rackwitz and Fiessler, 1978) is adopted for nonnormal random variables to estimate the equivalent normal distribution.

The sensitivity of the PMID with respect to the random variables is required for iteration procedures of the HL-RF algorithm. The direct differentiation method is utilized to compute the sensitivity of the PMID. Detailed formulations of the sensitivity for the PMID with respect to the random variables are derived in references (Kim et al., 2015 and Kim and Lee, 2017).

3 APPLICATIONS TO RC PYLONS

The reliability analyses are performed for the design sections of RC pylons for two cable-stayed bridges and one suspension bridge: The Incheon Bridge (IB), Busan Harbor Bridge (BHB), Yi Sun-shin Bridge (YSB), and New-millennium Bridge (NMB). Since the load combination under a strong wind condition without the live load governs the failure of the pylons, the dead and wind load effects are considered in the analyses.

The general view of the three cable-supported bridges and the longitudinal wind direction (WD) are presented in Figure 1. WD1 indicates the longitudinal wind direction acting on the left pylon to the right pylon, and WD3 designates the opposite wind direction of WD1. The front view of the pylons for the cable-supported bridges is illustrated in Figure 2, and the transverse wind directions denoted as WD2 and WD4 are indicated with the arrows at the top of each pylon in the figure. The transverse wind load is applied to both columns of a pylon simultaneously. Each pylon consists of two symmetric columns, and the reliability analysis is conducted for the bottom section of the left column for a pylon marked with a dotted circle in Figure 2.

Figure 3 shows the geometry and arrangement of reinforcements of the cross-section at the bottom of the pylons. Since the member axis of each column of the pylons is inclined from the vertical line, the cross-sections shown in Figure 3 are projected to the plane perpendicular to the member axis and marked with a dotted line in Figure 2 for the reliability analysis. The inclined angle of the column and sectional properties of the bottom sections of the pylons are

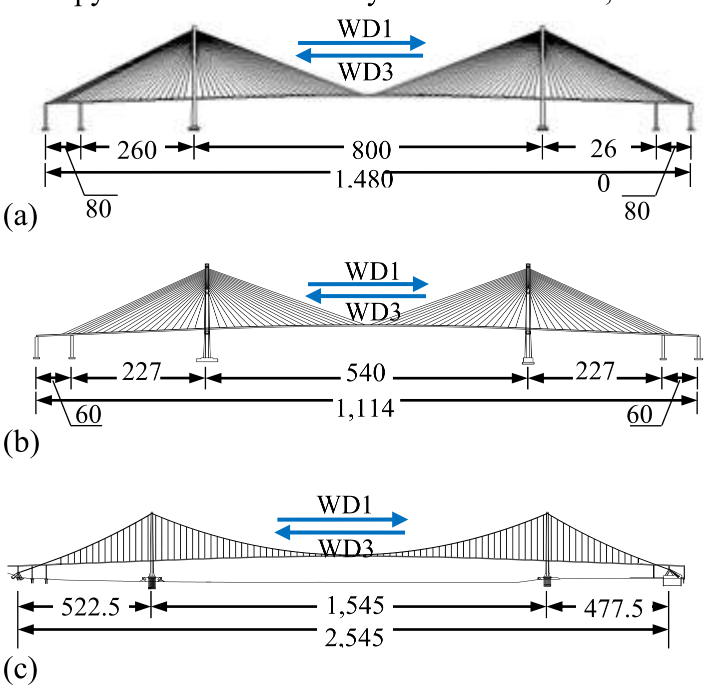

Figure 1. General view of cable-supported bridges and longitudinal wind direction: (a) IB; (b) BHB; (c) YSB (Unit: m)

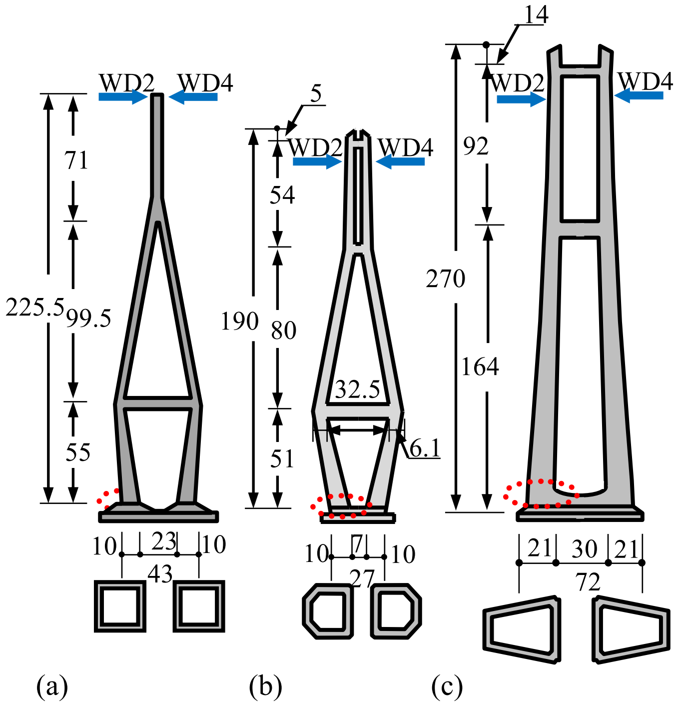

Figure 2. Front view of the pylon and transverse wind load direction: (a) IB; (b) BHB; (c) YSB (Unit: m)

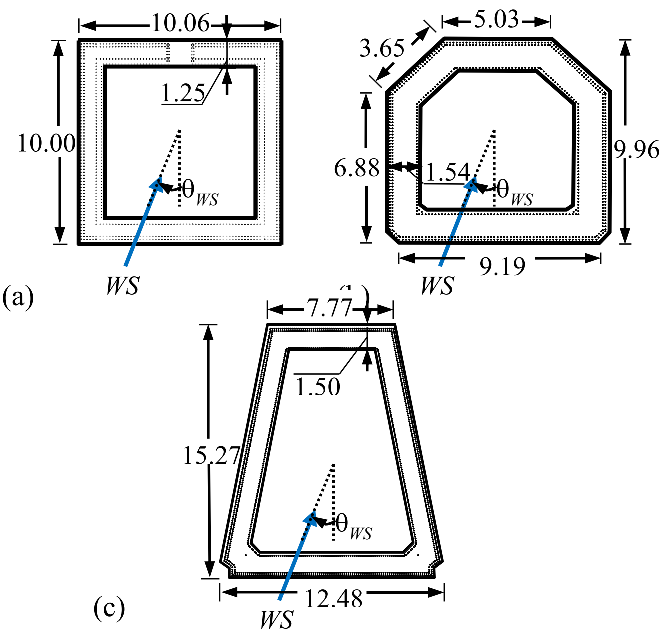

Figure 3. Geometry and rebar arrangement of the bottom section for the pylon: (a) IB; (b) BHB; (c) YSB (Unit: m)

summarized in Table 1. The nominal values of the compressive strength of concrete and the yield strength and Young's modulus of the reinforcements are also provided in the table. The reinforcement ratio of the cross-section where the lowest reliability index satisfies the target reliability index of 3.1 for λ_{WS} = 1, δ_{WS} = 0.3 is quoted from Kim et al. (2017), and is summarized for the three bridges in the table.

The statistical parameters of the random variables are given in Table 2 and quoted from the previous works (Kim et al., 2015; Kim et al., 2017). DC_P, DC_G, DC_C, DW, and WS indicate the dead load due to the self-weights of the pylons, girders, cable members, wearing surfaces and utilities, and the wind load, respectively.

The load effects induced by each load parameters are calculated using a commercial program, and are presented in Tables 3 and 4 for the longitudinal and transverse directions, respectively. WD in parentheses refers to the wind load direction illustrated in Figures 1 and 2. The calculated load effects include a moment amplification effect in axial forces and bending moment due to the P-delta effect. In the tables, the compression depicts a positive sign. The positive bending moments in the longitudinal and transverse directions represent the clockwise action in Figure 1 and the counterclockwise action in Figure 2, respectively.

Table 1. Inclined angle of the pylons and sectional properties of the sections

Bridge	Inclined angle	A_{gt}	Rebar ratio	f_{ck}	f_y	E_s
	(°)	(m^2)	(%)	(MPa)	(MPa)	(GPa)
IB	6.18	36.16	1.84	45	400	
BHB	12.14	47.48	0.52	40	400	200
YSB	3.22	69.35	0.46	40	400	

Table 2. Statistical parameters of the random variables

Random variable		Nominal value	Bias factor	COV	Distribution type
Material properties	f_{ck}	40/45MPa	1.15/1.16	0.10/ 0.095	Lognormal
	f_y	400/500MPa	1.15/1.09	0.08/ 0.05	Lognormal
	E_s	200GPa	1.00	0.06	Lognormal
Geometric properties	$A_{s,avg}$	-	1.00	0.015	Normal
	$\eta_{s,avg}$	0.00	1.00	-	Normal
	A_{gt}	-	1.01	0.056	Normal
Load parameters	DC_P	1.00	1.05	0.10	Normal
	DC_G	1.00	1.03	0.08	Normal
	DC_C	1.00	1.00	0.06	Normal
	DW	1.00	1.00	0.25	Normal
	WS	1.00	1.00	0.30	Gumbel

Table 3. Load effect matrices in the longitudinal direction

Bridge	Load effect	Load effect matrix					
		DC_P	DC_G	DC_C	DW	WS (WD1)	WS (WD3)
IB	P_q(MN)	115.9	82.0		30.4	0.8	-0.8
	M_q(MN·m)	0.0	87.2		-81.9	375.9	375.9
BHB	P_q(MN)	124.3	96.0		17.8	6.0	-5.9
	Mq(MN·m)	0.0	-63.4		79.7	596.8	596.8
YSB	P_q(MN)	271.7	95.3	51.3	28.1	2.5	-2.5
	M_q(MN·m)	0.0	-798.5	1008.0	-209.0	653.0	653.8

Table 4. Load effect matrices in the transverse direction

Bridge	Load effect	Load effect matrix					
		DC_P	DC_G	DC_C	DW	WS (WD2)	WS (WD4)
IB	P_q(MN)	115.9	82.0		30.4	-59.1	36.1
	M_q(MN·m)	-118.7	-25.6		-23.6	800.7	-782.9
BHB	P_q(MN)	124.3	96.0		17.8	-29.6	29.7
	Mq(MN·m)	-124.3	-23.1		-2.7	535.9	-525.4
YSB	P_q(MN)	271.7	95.3	51.3	28.1	-112.5	65.2
	M_q(MN·m)	255.0	50.0	9.9	14.8	2023.0	-1304.1

The angle of attack of the wind load to the pylon, θ_{WS}, is indicated in Figure 3. The angle of θ_{WS} = 0°, 90°, 180° and 270° correspond to WD1, WD2, WD3, and WD4, respectively. The angle of attack of the wind load varies from 0° to 360° while the nominal magnitude of the wind load is maintained constant. The effect of the surface exponent and the angle of attack on the results of the reliability analysis is investigated. For α = 2, the reliability analysis is performed with an interval of 5° for the angle of attack of wind load. The interval for the angle of attack for α = 1 is defined as 1° in order to clearly illustrate the discontinuity of the reliability indexes later on the figures.

The variations of the reliability indexes and the standard normal wind load at the failure point with the angle of attack for IB are presented in Figures 4 and 5, respectively. The variation patterns of the two figures are quite similar to each other, which implies that the wind load governs the failure of the pylon for the biaxial loads. The reliability levels of α = 2 are higher than the target reliability level for all the angle of attack, which is exactly the same for the other bridges. The lowest reliability index of α = 1 is calculated as 2.98 close to the WD2, which is 4% smaller than the target reliability index. Since the failure surface of the pylon is linearly interpolated in the case of α = 1, the strength of the pylon for biaxial bending decreases sharply and results in a lower reliability level.

Figure 6 shows the nominal load effects and the failure points for IB with respect to $0^\circ \leq \theta_{WS} \leq 360^\circ$, which are marked with centered symbols every 5° or 1° in a counter-clockwise direction. The solid squares in the figure indicate the internal forces at $\phi = 0°$, while the solid circles are associated with $\theta_{WS} = 90°$, 180° and 270°.

The axial forces corresponding to each centered symbol are different, and the load effects are located on different M_y-M_z planes in 3D space. Since the dead and wind loads generate the bending moments in the opposite and same directions in WD2 and WD4, respectively, the position of a large circle constructed with black blank circles, which present the nominal load effects, is shifted above the axis of $M_y = 0$. The results clearly show that the angles of attack for the failure points on the moment axes in Figure 6 exactly coincide with those where the discontinuities of $\alpha = 1$ and are observed in Figures 4 and 5. The re liability index of the pylon is calculated for uniaxial bending corresponding to $\theta_{WS} = 0°$, 90°, 180° and

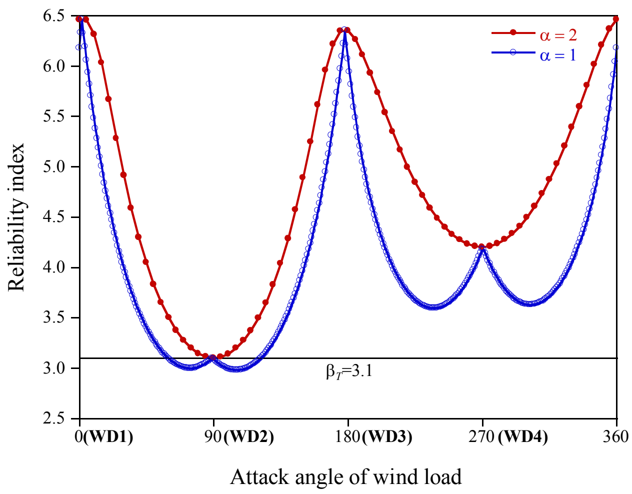

Figure 4. Reliability indexes of pylons for IB under biaxial bending

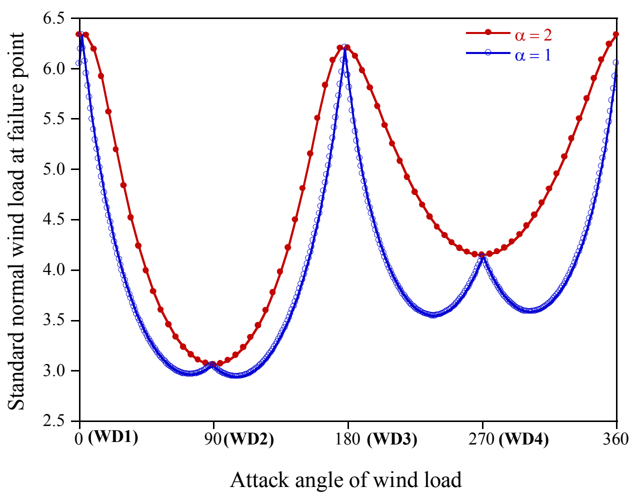

Figure 5. Standard normal wind load at the failure point of pylons for IB under biaxial bending

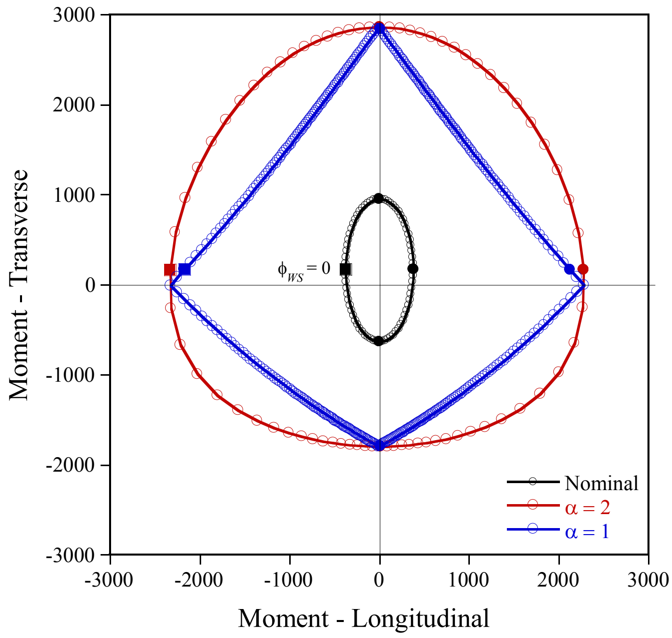

Figure 6. Nominal bending moments for IB

270° and is compared with that for biaxial bending in Table 5. The bending moments about the axis perpendicular to the wind load and the axial forces given in Tables 3 and 4 are considered for uniaxial bending. A slight difference in the reliability indexes between uniaxial bending and biaxial bending is caused by the biaxial moment due to the dead load.

Since the wind loads in WD2 and WD4 induce the tensile and compressive axial forces, respectively, the pylon under the load effects in WD4 exhibits a higher level of safety than that in WD2 even though the total nominal moment in WD4 is larger than that in WD2. This is because the moment capacity of a pylon decreases rapidly as the compressive axial force diminishes in the tensile failure region of the PMID. The longitudinal wind load yields a similar level of reliability indexes in WD1 and WD3. As in the transverse wind load case, the difference in the reliability indexes in WD2 and WD4 is caused by the opposite wind load effect on the axial forces of the pylons. However, the axial forces induced in the pylons by the longitudinal wind load are much smaller than those by the transverse wind load, which leads to a less significant difference in the reliability indexes between the two longitudinal

Table 5. Comparison of reliability indexes under uniaxial and biaxial bending for IB

Wind direction	Reliability index	
	Uniaxial bending	Biaxial bending ($\alpha = 2$)
WD1	6.47	6.46
WD2	3.10	3.10
WD3	6.36	6.35
WD4	4.20	4.20

wind load cases in comparison to the transverse wind load case. The reliability index seems to be proportional to the distance between the nominal load effect and the failure point as shown in Figures 4 and 6. However, it should be noted that such a proportional relationship may not be valid according to the failure mode of a pylon depending on the load combination (Kim et al., 2015).

Figures 7 and 8 show the reliability indexes and the standard normal wind load at the failure point for BHB under biaxial bending, respectively. The comparison of reliability indexes for uniaxial and biaxial bending is presented in Table 6, and the nominal load effects and the failure points in M_y–M_z space are illustrated in Figure 9. The smallest reliability index is calculated in WD2 for both uniaxial bending and biaxial bending of α = 2. However, the lowest reliability level of α = 1 is calculated as 2.21 at θ_{WS} = 215°, and the reliability indexes of α = 1 decreases more rapidly in the range of $180^\circ \le \theta_{WS} \le 360^\circ$ than at $0^\circ \le \theta_{WS} \le 180^\circ$. The large biaxial moments are generated in the range of $180^\circ \le \theta_{WS} \le 360^\circ$ by the superposition of the bending moment in the longitudinal and transverse direction, and are very close to the failure surface of α = 1. The combination of bending moments with a short distance to the failure surface yields a higher probability of failure.

The comparison of reliability indexes for uniaxial and biaxial bending is presented in Table 6. Since the ratio of bending moment due to the dead load to the wind load is apparently large in comparison with the other bridges (*vide* Tables 3 and 4), the failure points for biaxial bending exist within the quadrant and not on the axes. The reliability levels for uniaxial bending are a little bit higher than those for biaxial loads in WD1, WD3, and WD4 for α = 2 as shown in Table 6.

The results of the reliability assessment for YSB are presented in Figures 10-12, and Tables 7. Discussions on the results of the YSB are similar to those of IB. For YSB the bending moments due to the dead and wind load are produced in the same

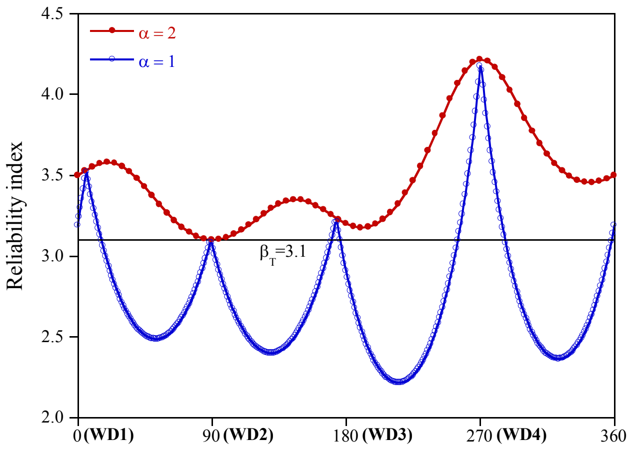

Figure 7. Reliability indexes of pylons for BHB under biaxial bending

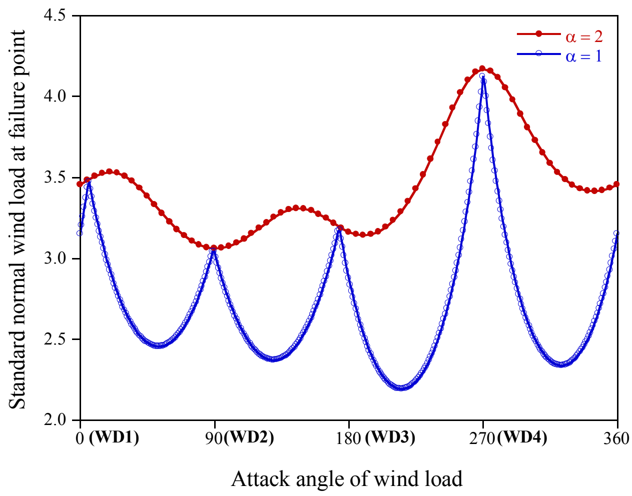

Figure 8. Standard normal wind load at the failure point for BHB under biaxial bending

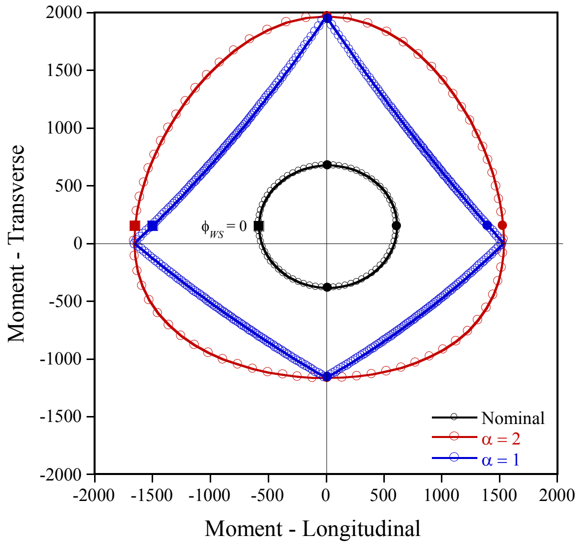

Figure 9. Standard normal wind load at the failure point for BHB under biaxial bending

Table 6. Comparison of reliability indexes under uniaxial and biaxial bending for BHB

Wind direction	Reliability index	
	Uniaxial bending	Biaxial bending (α = 2)
WD1	3.51	3.50
WD2	3.10	3.10
WD3	3.21	3.20
WD4	4.27	4.22

transverse direction. Thus, the unions of the nominal load effects are positioned below the axis of M_y = 0 as shown in Figure 12. In the three bridges, the minimum reliability indexes for biaxial bending are lower than that for uniaxial bending by 4% to 28% and are summarized in Table 8. Therefore, even if a pylon secures a high reliability level for uniaxial bending, a significantly lower reliability level may result for biaxial bending, which depends on the surface exponent.

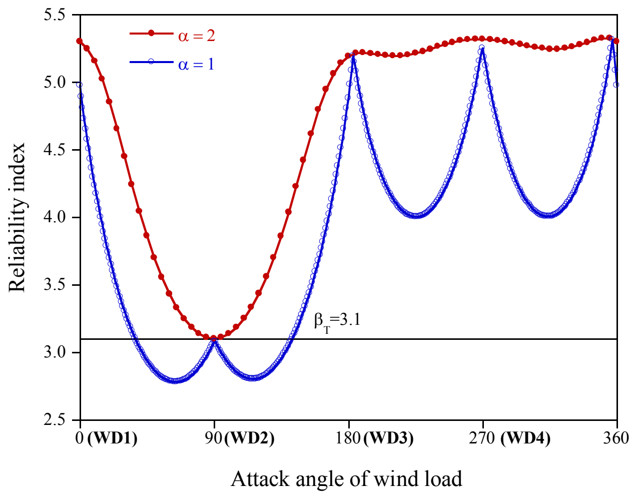

Figure 10. Reliability indexes of pylons for YSB under biaxial bending

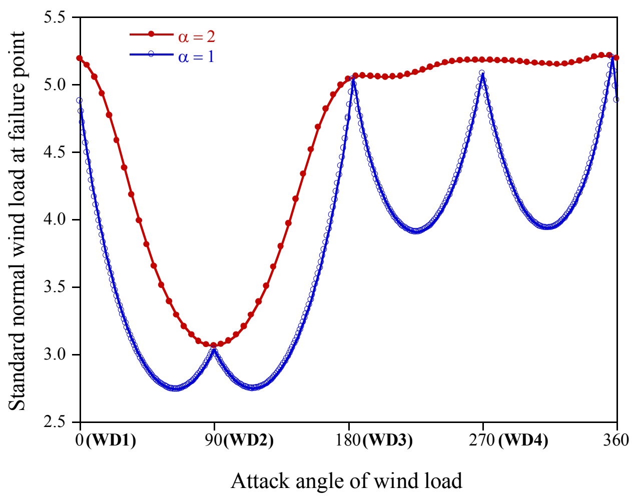

Figure 11. Standard normal wind load at the failure point for YSB under biaxial bending

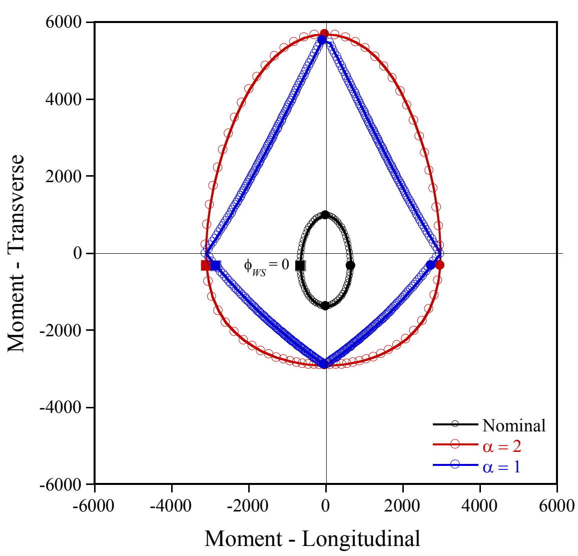

Figure 12. Nominal bending moments for YSB

Table 7. Comparison of reliability indexes under uniaxial and biaxial bending for YSB

Wind direction	Reliability index	
	Uniaxial bending	Biaxial bending (α = 2)
WD1	5.32	5.30
WD2	3.10	3.10
WD3	5.20	5.19
WD4	5.32	5.32

Table 8. Minimum reliability index of pylons of five bridges (α = 1)

Bridge	Angle of attack (°)	Minimum reliability index	Difference with target reliability index (%)
IB	106	2.98	3.9
BHB	215	2.22	28.4
YSB	64	2.78	10.3

4 CONCLUSIONS

This paper presents the reliability assessment of RC pylons for three cable-supported bridges in Korea. The failure surface of RC pylons is defined by the load contour method. The load and strength parameters are considered as random variables. The reliability analysis is performed for the section of which the lowest reliability index secures a certain target reliability index. The surface exponents of the load contours are used as 1 and 2 in order to calculate the reliability index for the lower and upper limits of the strength.

The limit state of a pylon is mainly governed by the wind load. The reliability level for surface exponent of 1 is higher than the target reliability index of 3.1 for all angle of attack. The minimum reliability index under biaxial bending for surface exponent of 1 is reduced by 4-28% of the target reliability index. Since the reliability index for biaxial loads varies significantly with the surface exponent, most design codes specify the surface exponent as one in order to deduce conservative design. The precise surface exponent for a cross-section is required for more economical design.

ACKNOWLEDGEMENTS

This research was supported by a grant (17SCIP-B119964-02-000000) from the Ministry of Land, Transport and Maritime Affairs of the Korean government through the Korea Bridge Design & Engineering Research Center of Seoul National University.

REFERENCES

AASHTO (American Association of State Highway and Transportation Officials). 2014. *AASHTO LRFD Bridge Design Specifications*, Washington, DC.

Haldar, A., & Mahadevan, S. 2000. *Probability, Reliability and Statistical Methods in Engineering Design,* John Wiley & Sons, Inc., New York, 181-224.

Kim, J. H., Lee, S. H., Paik, I., and Lee, H. S. 2015. "Reliability assessment of reinforced concrete columns based on the P-M interaction diagram using AFOSM." *Struct. Safety*, 55, 70-79.

Kim, J. H., & Lee, H. S. 2017. "Reliability assessment of reinforced concrete columns subjected to biaxial bending using the load contour method." *Engineering Structures*, 150, 636-645.

Kim, J. H., Yoo, C-H., and Lee, H. S. 2017. "Evaluation of wind load factors of RC columns for wind load-governed limit stat in reliability-based design code." *Journal of Bridge Engineering, ASCE*, 22(9): 04017053.

KMOLIT (Korea Ministry of Land, Infrastructure and Transport). 2016a. *Korean Highway Bridge Design Code* (*Limit State Design*), KMOLIT, Seoul.

KMOLIT (Korea Ministry of Land, Infrastructure and Transport). 2016b. *Korean Highway Bridge Design Code (Limit State Design) – Cable Supported Bridges*, KMOLIT, Seoul.

Kreyszig, E. 2006. *Advanced Engineering Mathematics*, 9th ed., John Wiley & Sons, Inc.

Liu, P. L., and Der Kiureghian, A. 1991. Optimization algorithms for structural reliability. *Structural Safety*, 9, 161-177.

Rackwitz, R., & Fiessler, B. 1978. "Structural reliability under combined random load sequences." *Comput. Struct.*, 9(5), 489-494.